Homann, P. H. (1989) in *The Role of Calcium in Biological Systems*, Vol. V, CRC Press, Boca Raton, FL (in press).
Isawa, S., Heath, R. L., & Hind, G. (1969) *Biochim. Biophys. Acta 180*, 388-398.
Itoh, S., Yerkes, C. T., Koike, H., Robinson, H. H., & Crofts, A. R. (1984) *Biochim. Biophys. Acta 766*, 612-622.
Kok, B., Forbush, B., & McGloin, M. (1970) *Photochem. Photobiol. 11*, 457-475.
Krogmann, D. W., Jagendorf, A. T., & Avron, P. (1959) *Plant Physiol. 34*, 272-275.
Ono, T.-A., & Inoue, Y. (1988) *Arch. Biochem. Biophys. 264*, 82-92.
Ono, T.-A., Zimmermann, J.-L., Inoue, Y., & Rutherford, A. W. (1986) *Biochim. Biophys. Acta 851*, 193-201.
Pecoraro, V. L. (1988) *Photochem. Photobiol. 48*, 249-264.
Radmer, R., & Ollinger, O. (1986) *FEBS Lett. 195*, 285-289.
Rutherford, A. W. (1989) *Trends Biochem. Sci. 14* (6), 227-232.
Rutherford, A. W., & Zimmermann, J.-L. (1984) *Biochim Biophys. Acta 767*, 168-175.
Sandusky, P. O., & Yocum, C. F. (1983) *FEBS Lett. 162*, 339-343.
Sandusky, P. O., & Yocum, C. F. (1984) *Biochim. Biophys. Acta 766*, 603-611.
Sandusky, P. O., & Yocum, C. F. (1986) *Biochim. Biophys. Acta 849*, 85-93.
Sivaraja, M., & Dismukes, G. C. (1988) *Biochemistry 27*, 3467-3475.
Styring, S., & Rutherford, A. W. (1988) *Biochim. Biophys. Acta 933*, 378-387.
Theg, S. M., Jursinic, P. A., & Homann, P. H. (1984) *Biochim. Biophys. Acta 766*, 636-646.
Thompson, L. M. (1989) Ph.D. Thesis, Yale University.
Velthuys, B. R. (1975) Thesis, University of Leiden.
Vernon, L. P., & Zaug, W. S. (1960) *J. Biol. Chem. 235*, 2728-2733.
Yocum, C. F., & Babcock, G. T. (1981) *FEBS Lett. 130*, 99-102.
Zankel, K. L. (1971) *Biochim. Biophys. Acta 245*, 373-385.
Zimmermann, J.-L., & Rutherford, A. W. (1984) *Biochim. Biophys. Acta 767*, 160-167.
Zimmermann, J.-L., & Rutherford, A. W. (1986) *Biochemistry 25*, 4609-4615.

Kinetics of Calcium Channel Opening by Inositol 1,4,5-Trisphosphate†

Tobias Meyer, Theodore Wensel,‡ and Lubert Stryer*
Department of Cell Biology, Sherman Fairchild Center, Stanford University School of Medicine, Stanford, California 94305
Received June 20, 1989; Revised Manuscript Received August 10, 1989

ABSTRACT: The subsecond mobilization of intracellular Ca^{2+} by IP_3 was measured with rapid mixing techniques to determine how cells achieve rapid rises in cytosolic [Ca^{2+}] during receptor-triggered calcium spiking. In permeabilized rat basophilic leukemia cells at 11 °C, more than 80% of the 0.7 fmol of Ca^{2+}/cell sequestered by the ATP-driven pump could be released by IP_3. Half of the stored Ca^{2+} was released within 200 ms after addition of saturating (1 μM) IP_3. The flux rate was half-maximal at 120 nM IP_3. Ca^{2+} release from fully loaded stores was highly cooperative; the Hill coefficient over the 2-40 nM range was greater than 3. The delay time of channel opening was inversely proportional to [IP_3], increasing from 150 ms at 100 nM IP_3 to 1 s at 15 nM, indicating that the rate-limiting step in channel opening is IP_3 binding. Multiple binding steps are required to account for the observed delay and nonexponential character of channel opening. A simple model is proposed in which the binding of four IP_3 molecules to identical and independent sites leads to channel opening. The model agrees well with the data for K_D = 18 nM, $k_{on} = 1.2 \times 10^8$ M^{-1} s^{-1}, and k_{off} = 2.2 s^{-1}. The ~1-s exchange time of bound IP_3 indicates that the channel gating sites are distinct from binding sites having ~100-s exchange times that were previously found with radiolabeled IP_3. The ~1-s response time of [Ca^{2+}] to a rapid increase in IP_3 level can account for observed rise times of calcium spikes.

Many hormones, neurotransmitters, and other extracellular stimuli activate the phosphoinositide cascade by binding to cell surface receptors that are coupled to phospholipase C. The subsequent increase in inositol 1,4,5-trisphosphate (IP_3) leads to Ca^{2+} release from intracellular stores (Berridge, 1987; Carafoli, 1987; Putney, 1987). Recent studies indicate that receptor-triggered Ca^{2+} release is often pulsatile rather than sustained. Activated cells exhibit repetitive transient increases in cytosolic Ca^{2+} (Woods et al., 1986; Miyazaki et al., 1986; Jacob et al., 1988). A mechanistic understanding of Ca^{2+} spiking requires detailed knowledge of the kinetics of IP_3-induced Ca^{2+} release. In previous studies with permeabilized rat basophilic leukemia cells (RBL cells), we found that the IP_3-gated Ca^{2+} channel is cooperatively opened by IP_3 with a Hill coefficient of 2.7 (Meyer et al., 1988). Because the time resolution of our earlier study was 4 s, the kinetics of release under physiological IP_3 conditions could not be measured. We report here rapid-kinetic studies of IP_3-induced Ca^{2+} release having a time resolution of 10 ms. The observed dependence of release kinetics on nanomolar IP_3 concentration in the

† This work was supported by grants from the National Institute of General Medical Sciences (GM24032 and GM30387), a Swiss National Science Foundation Fellowship (to T.M.), and an NIH postdoctoral fellowship (EY05815 to T.W.).
‡ Present address: Department of Biochemistry, Baylor College of Medicine, One Baylor Plaza, Houston, Texas 77030.

0006-2960/90/0429-32$02.50/0

subsecond time range gives insight into the channel gating process. These experiments provide information concerning the minimum number of IP_3-binding sites that control channel opening, the number of delay steps in channel opening, microscopic on-rates and off-rates from the channel gating sites, and the transition time between occupancy of the receptor and channel opening.

Materials and Methods

Materials. The following were purchased: Inositol 1,4,5-trisphosphate (IP_3) from Sigma or Calbiochem, diethylenetriaminepentaacetic acid anhydride (DTPA) and calcium-indicating dyes (fluo-3, fura-2, and rhod-2) from Molecular Probes, and aminoethyl Bio-Gel P-2 from Bio-Rad.

Buffer. The standard buffer for flux measurements contained 20 mM HEPES (pH 7.4), 145 mM KCl, 5 mM NaCl, 2 mM Mg^{2+}, and 0.7 mM ATP.

Preparation of Chelating Resin ("Ca^{2+} Sponge"). Removal of contaminating metal ions is necessary to achieve the improved Ca^{2+}-release sensitivity described here. Because a commercially available chelating resin (Chelex 100, Bio-Rad) did not sufficiently lower metal ion contamination from solutions of Ca^{2+} indicator dyes, we prepared a heptadentate DTPA-based resin that binds metal ions much more strongly. DTPA anhydride (12 g, 33.6 mmol) was suspended in a mixture of 100 mL of DMSO and 400 mL of glacial acetic acid. Sixteen grams (nominally 1.1 mmol of amino groups) of dry aminoethyl Bio-Gel P-2 was added. The mixture was stirred and refluxed for 4 h at 131 °C. The resin was filtered and washed with DMSO twice, 0.1 N NaOH twice, 0.1 N HCl twice, and 100 mL of H_2O. When equilibrated with the standard flux assay buffer, the resin had a Ca^{2+}-binding capacity of 145 μmol of Ca^{2+}/mL of wet resin. When Ca^{2+} removal efficiency decreased after repeated use, the resin was regenerated by using 0.1 N HCl.

Removal of Metal Contamination from Buffers, Stock Solutions, and Exposed Surfaces. Labware (all plastic) was washed with detergent, followed by 0.1 N HCl, distilled water, and finally the buffer to be used (containing dye where appropriate). All solutions were passed over the Ca^{2+} sponge. Using the Ca^{2+} indicator fluo-3, all solutions, cuvettes, and stir bars were tested for contaminating metal ions before use. In a typical fluorescence experiment, 3–20 μL of a stock (e.g., IP_3, ATP, glucose) was added to 2 mL of stirred sample.

Preparation of Rat Basophilic Leukemia Cells. RBL cells [2×10^7 cells, grown as described Taurog et al. (1979)] were harvested at days 4–5 and diluted into 16 mL of a Ca^{2+}- and Mg^{2+}-free buffer containing 20 mM HEPES (pH 7.4), 140 mM NaCl, and 5 mM KCl. Cell pellets were washed twice by centrifugation with the same buffer and the third time with the final standard buffer containing 1–1.5 μM metal-free fluo-3. The cells were permeabilized with 85 μg/mL Ca^{2+}-free saponin for 10 min at room temperature, in the presence of 2 mM Mg^{2+} and 0.7 mM ATP to ensure reloading of Ca^{2+} that had leaked out of the IP_3-sensitive store.

Fluorescence Measurements. The fluorescence of fluo-3 was measured by using an SLM-8000 fluorimeter interfaced to an IBM PC and equipped with a band-pass filter (rather than a monochromator) on the emission side. For experiments not requiring subsecond time resolution, measurements were made in a 1-cm acrylic cuvette (Sarstedt) containing 2 mL of buffer and a Teflon stir bar. The fluorescence signal was corrected for fluctuations in excitation light intensity. The concentration of free Ca^{2+}, $[Ca^{2+}]$, was determined from the fraction of dye bound, $f = (I - I_E)/(I_C - I_E)$, by

$$[Ca^{2+}] = K_D f/(1 - f) \quad (1)$$

where K_D is the apparent dissociation constant, I_C is the fluorescence due to the high-affinity Ca^{2+}-binding site of fluo-3 when fully saturated, and I_E is the fluorescence intensity in the absence of bound Ca^{2+} (i.e., with excess EGTA). Total Ca^{2+}, Ca^{2+}_{tot}, is given by

$$Ca^{2+}_{tot} = fD_{tot} + [Ca^{2+}] \quad (2)$$

where D_{tot} is the total added dye, typically 1 μM. Titrations of metal-free fluo-3 with Ca^{2+} indicated a high-affinity binding site with K_D = 600 nM in buffer B and an apparent additional site with K_D = 200 μM (data not shown). Because the second site gave rise to an intensity increase equal to 0.14 that due to the high-affinity site, I_C was calibrated by adding Ca^{2+} to a total of 33 μM in each sample following a flux experiment. I_E was then calibrated by adding EGTA to 5 mM. To facilitate comparison of our results with those of other laboratories, we used the value K_D = 450 nM given by Molecular Probes (Eugene, OR). The sensitivity of the system was tested by additions of known amounts of Ca^{2+}.

Calibration and Sensitivity of the Calcium-Flux Assay. Elimination of heavy metals and Ca^{2+} by treatment of the buffer with the Ca^{2+} sponge allowed the Ca^{2+} indicator fluo-3 to be the major Ca^{2+} buffer, providing reliable detection of nanomolar Ca^{2+} fluxes. Assays requiring EGTA buffering dampen the indicator response because most of the released Ca^{2+} does not bind to fluo-3. Similarly, when larger indicator concentrations are used, the fractional signal change due to released Ca^{2+} is small. In a system where the indicator dye is the only significant Ca^{2+} buffer, the sensitivity to added Ca^{2+} is given by

$$\Delta f/[Ca^{2+}]_{added} = [D_{tot} + K_D/(1 - f)^2]^{-1} \quad (3)$$

This relationship has been experimentally verified for fluo-3 (and also for fura-2 and rhod-2). The assay is most sensitive at $[Ca^{2+}]$ values below K_D, and practical considerations (instrumental and scattering noise contributions) make the assay most useful for different indicators in the following free $[Ca^{2+}]$ ranges: fura-2, 10–250 nM; fluo-3, 20–450 nM; and rhod-2, 40–1000 nM. The limits on sensitivity are set by the intrinsic instrumental noise (here 0.03%, primarily due to the amplifier) and light scattering from cellular components (typically 0.1%).

An important consequence of the improved sensitivity of this assay is the ability to work at high cell dilutions, where intracellular volume represents only 0.05%–0.1% of total sample volume. This dilution of cytoplasmic enzymes minimizes the degradation of IP_3 by endogenous phosphatases. Under the conditions employed here, IP_3 is degraded to IP_2 with first-order kinetics. HPLC analysis following incubation of permeabilized cells with $[^3H]IP_3$ showed that the half-life is greater than 600 s (Meyer & Stryer, 1988). Conversion to IP_4 occurs at an even slower rate. Because IP_2 and IP_4 do not alter Ca^{2+} fluxes at the concentrations present in these experiments (Meyer et al., 1988), their formation can be ignored in interpreting the present data. The concentration of IP_3 is nearly constant during the time course of the experiments reported here. Likewise, because ATP only affects the uptake and not the release of Ca^{2+}, it is unlikely that modulation of the channel by kinases occurs in our permeabilized cell system.

Rapid Mixing. A stopped-flow apparatus (SFA-11, High Tech Scientific, Salisbury, U.K.) was used for rapid mixing of permeabilized cells and IP_3. Mixing occurred approximately 25 ms before the triggering of the fast data acquisition mode of the SLM 8000, as estimated from test experiments with fluo-3, Ca^{2+}, and EGTA. The fluo-3 response is faster than 25 ms. To obtain enhanced intensity, the sample was excited with the 488-nm line of an air-cooled argon ion laser (Ion

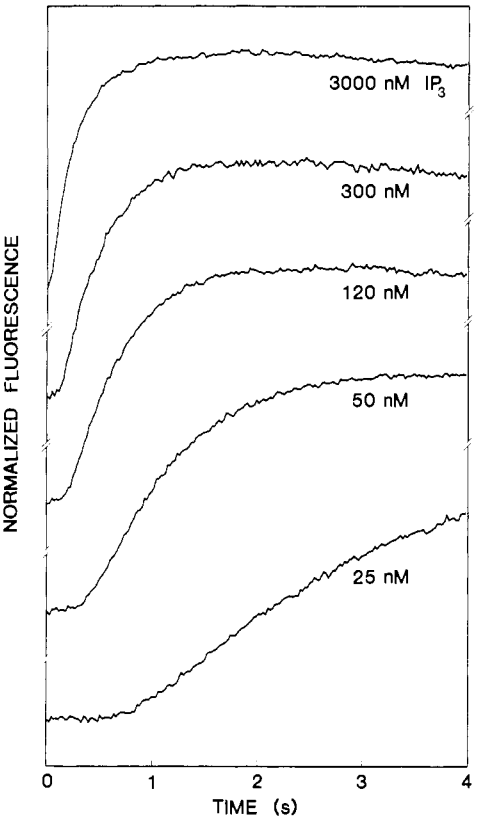

FIGURE 1: Rapid kinetics of IP_3-gated Ca^{2+} release. The fluo-3 fluorescence intensity monitors the release of Ca^{2+} induced by rapidly mixing permeabilized cells with the indicated concentrations of IP_3. The concentration of free Ca^{2+} increased from a value of about 250 nM to 450 nM. The time axis begins during mixing. Ca^{2+} release approximately follows first-order kinetics after a concentration-dependent lag time.

Laser Technology). Integration times of 11 or 22 ms were used for the fluorescence recording.

Results and Discussion

Ca^{2+}-Efflux Rates as a Function of IP_3. The kinetics of IP_3-induced Ca^{2+} release were measured with a stopped-flow device. RBL cells permeabilized in the presence of Mg^{2+}/ATP (10 min at room temperature) were loaded in one syringe of the rapid mixing device while the other syringe was filled with the same buffer (with Mg^{2+}/ATP) containing IP_3. Typical rapid mixing results obtained at 11 °C with a concentration of 6×10^5 cells/mL are shown in Figure 1. Released Ca^{2+} binds fluo-3 and increases its fluorescence, whereas Ca^{2+} sequestered in the intracellular store is not exposed to this indicator. The fluorescence increase was nearly linear with the Ca^{2+} released in the free Ca^{2+} range of 150–250 nM (for details and calibration, see Materials and Methods). Varying the free Ca^{2+} concentration from 150 to 800 nM did not significantly affect the release kinetics. In contrast, the $[IP_3]$ dependence of channel opening was strongly altered by pH. Threefold less IP_3 was required at pH 8 than at pH 7.4, and eight-fold more at pH 6, for the opening of the same amount of channels. Maximal loading in the presence of Mg^{2+}/ATP was determined to be 0.7 fmol/cell. At a saturating IP_3 concentration, half of the Ca^{2+} (0.35 fmol/cell) was released after 200 ms, corresponding to a maximal efflux rate of 1.75 fmol/(cell·s) (the 3000 nM trace in Figure 1). This rate corresponds to a flux of 1.05×10^9 Ca^{2+} ions/(s·cell) or an intracellular Ca^{2+} current of 0.34 nA. At 25 nM IP_3, half-depletion of the Ca^{2+} store occurred in about 1 s after a 700-ms lag.

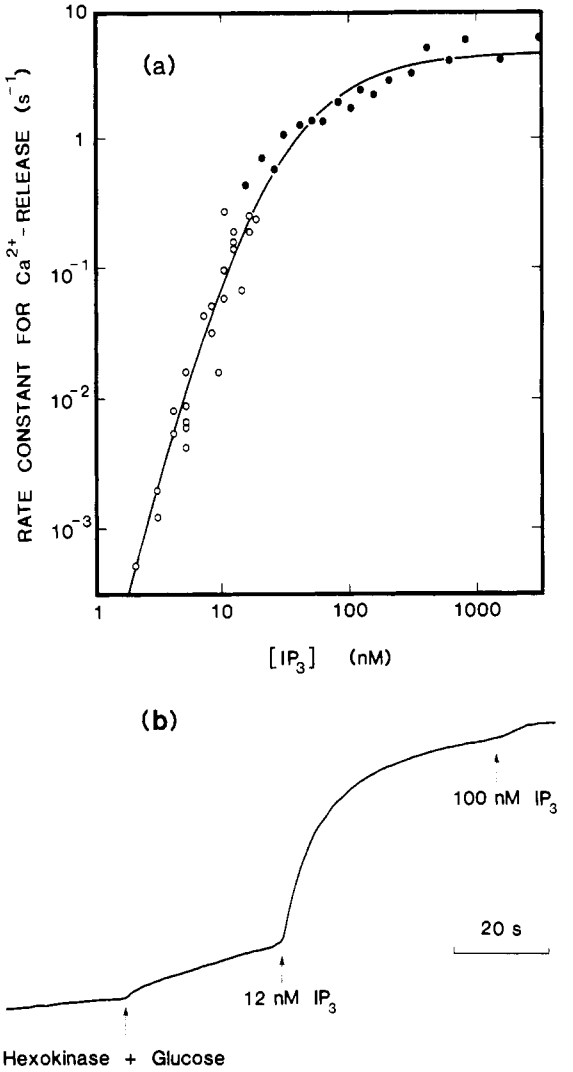

FIGURE 2: IP_3 dependence of the efflux rate constant. The rate constants (panel a) are defined as the reciprocal of the time required for half-maximal release of Ca^{2+} from the IP_3-sensitive store. The lag time before Ca^{2+} release was subtracted. Ca^{2+} efflux was measured by using the stirred-cuvette method for low IP_3 concentrations (raw data in panel b and open circles in panel a) and the rapid mixing technique for high IP_3 concentrations (filled circles in panel a). For low IP_3 concentrations, a mixture of hexokinase and glucose was added to eliminate ATP and stop Ca^{2+} pumping prior to IP_3 addition (panel b). The efflux rate was corrected for the slow leak observed after ATP depletion. The smooth curve in panel a is predicted for a four-site model described in the text, calculated according to the following equation: rate constant = $(5.5\ s^{-1})[c/c + 18\ nM)]^4$, where $c = [IP_3]$.

The efflux rate constants determined from the rapid mixing data are plotted as a function of $[IP_3]$ in the 10–3000 nM range in Figure 2a (solid circles). To obtain a better signal-to-noise ratio, the lower range of IP_3 concentrations was measured by using a standard cuvette instead of the stopped-flow cell. At IP_3 concentrations below about 10 nM, ATP-driven Ca^{2+} uptake becomes significant compared to IP_3-induced release. For this reason, the ATP level was lowered by addition of glucose (10 mM) and hexokinase (10 units/mL) shortly before addition of IP_3. Figure 2b shows a 12 nM IP_3 addition after pretreatment with glucose and hexokinase. A constant leak of the fully loaded store, measured in the absence of both ATP and IP_3, was subtracted from the efflux rate observed in the presence of IP_3. This procedure enabled us to measure efflux rate constants in the 2–25 nM concentration range (Figure 2a, open circles). At low IP_3 concentrations, the Hill coefficient is greater than 3. The efflux rate was

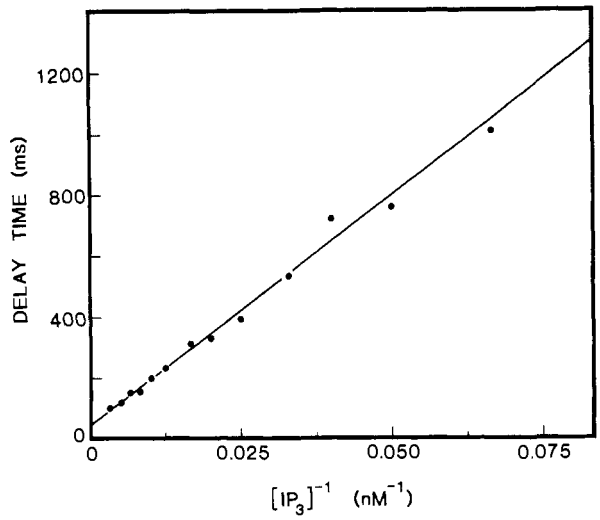

FIGURE 3: Delay times for channel opening. From a series of experiments similar to the ones shown in Figure 1, the time to reach a half-maximal slope was determined. This delay time is plotted versus $1/[IP_3]$. The linear fit of the data shows that the on-rate for IP_3 binding is $k_{on} = 4.6 \times 10^7$ M^{-1} s^{-1} if a single binding step is limiting. The y intercept (the delay time at saturating $[IP_3]$) is 65 ms.

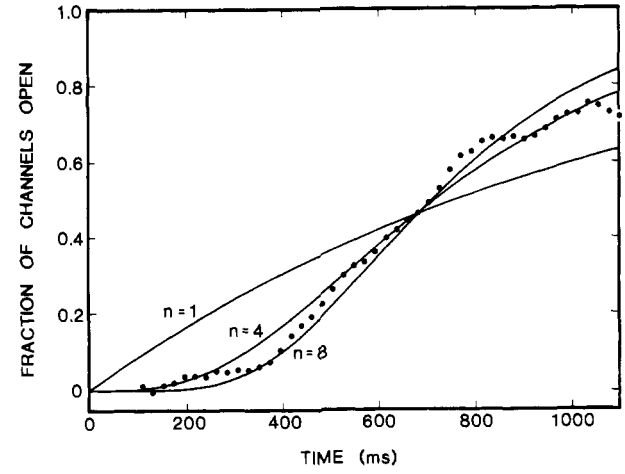

FIGURE 4: Time course of channel opening. The results from a series of 12 rapid mixing experiments at 30 nM final $[IP_3]$ were averaged (to reduce noise), and the first derivative was calculated. The data points correspond to the slope at intervals of 22 ms. The smooth curves are fits to the kinetic model described in the text with 1, 4, or 8 delay time constants. The data were corrected for a 5% fluorescence drift after mixing.

half-maximal at 120 nM IP_3. The results obtained in this way for low IP_3 concentrations are similar to those obtained previously (Meyer et al., 1988), in which IP_3-mediated Ca^{2+} flux was measured in cells whose Ca^{2+} stores were 90%–95% depleted. Thus, the steeply cooperative dependence on $[IP_3]$ is independent of the initial amount of Ca^{2+} in the intracellular stores.

Delay Times for Channel Opening. The maximal flux rate was not attained immediately upon mixing. Rather, a delay ranging from 65 ms to 1.5 s was observed (Figure 1). A series of rapid mixing traces was analyzed to determine the $[IP_3]$ dependence of the delay time for channel opening, which is defined as the time required to reach a half-maximal flux rate after IP_3 addition. Delay times increased with decreasing IP_3 concentrations from about 80 ms at 500 nM IP_3 to 1000 ms at 15 nM IP_3. As shown in Figure 3, there is a linear relationship between the delay time and the reciprocal of the IP_3 concentration. This result indicates that an IP_3-binding step is kinetically limiting for channel opening. In the simple case where diffusion is unhindered and binding of ligand to channel gating sites is rate-limiting, the delay time τ at a ligand concentration c is given by

$$\tau = 1/(k_{on}c) \text{ for } c \gg K_D \quad (4)$$

$$\tau = 1/k_{off} \text{ for } c \ll K_D \quad (5)$$

The slope of the straight-line fit through the data in Figure 3 corresponds to a k_{on} of 4.6×10^7 M^{-1} s^{-1} if the delay is due to a single binding site and to a k_{on} of 1.2×10^8 M^{-1} s^{-1} in the case of four IP_3-binding sites (see below). Because the plot is linear even at IP_3 concentrations as low as 20 nM, one of the binding steps for channel opening must have a $K_D <$ 20 nM. The y intercept of 65 ms (τ_0) indicates that there is an $[IP_3]$-independent delay in channel opening. This 65-ms delay may be the time required for opening of a fully liganded channel. Alternatively, the 65-ms delay may reflect the time required for diffusion of either IP_3 or Ca^{2+} across barriers between the intracellular stores and the extracellular space. In any event, opening of a fully liganded channel must occur in 65 ms or less.

Time Course of Channel Opening. Additional information can be obtained by analyzing the entire time course of channel opening, which is complex and nonexponential. To improve the signal-to-noise ratio, 12 traces recorded with a sampling interval of 11 ms were averaged. We analyzed the time course of Ca^{2+} store depletion after addition of 30 nM IP_3, measured as an increase in fluo-3 fluorescence (similar to Figure 1). In Figure 4 the first derivative of this curve, the rate of efflux, was assumed to be proportional to the number of open channels. This assumption holds, provided that the store is not substantially depleted and the fluorescent signal change is in the linear range. To ensure these conditions, only the first 1100 ms of the depletion process was analyzed. Linear least-squares fits over 200-ms intervals were used to determine the slope of the curve. Figure 4 plots the first derivative of the efflux curve, expressed as the fraction of final channel opening. Multiple slow lag times are necessary to account for the nonexponential delay evident in Figure 4. These data were fit to a series of model functions of the form $[1 - \exp(-t/\tau_n)]^n$ (derived from the model described below) with $n = 1$–8. Resulting τ_n's were 1155, 385, and 286 ms for $n = 1$, 4, and 8, respectively. Best agreement with the data could be obtained with $n \geq 4$. Values of n from 4 to 8 yielded equally good fits. Thus, multiple binding steps are required for channel opening.

Model for IP_3-Gated Channel Opening. Analysis of the kinetics of Ca^{2+} release provides three lines of evidence showing that multiple IP_3 binding events are required to open the Ca^{2+} channel: (1) The dependence of the efflux rate constant on $[IP_3]$ is steeply cooperative (Figure 2a). A best fit to the curve can be obtained for $n = 4$ (or 5). (2) The IP_3 concentration required for half-maximal channel opening, $K_{1/2} = 120$ nM (Figure 2a), is much greater than K_D for binding to one of the channel gating sites, for which an upper limit of 20 nM was inferred from the delay data as described above (Figure 3). A simple model with independent and equal binding that would explain this difference requires a cooperativity coefficient >4.5 [deduced from $[K_{1/2}/(K_{1/2} + K_D)]^n = 0.5$]. (3) There are multiple delay steps between a rise in ligand concentration and opening of the channel (Figure 4). Best fits were obtained for $n = 4$–8.

Although none of these three lines of evidences rigorously excludes a model with three gating sites, a better fit to the data is obtained by assuming that four or more molecules of IP_3 must be bound to a receptor before the channel can open. For simplicity, we assume four binding sites. Furthermore we assume that they are independent (i.e., the binding events themselves are not cooperative).

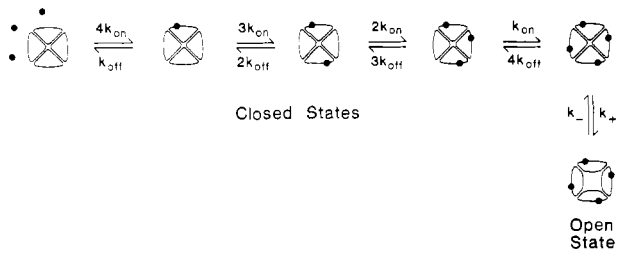

FIGURE 5: Model used to analyze the efflux kinetics: four independent IP_3-binding sites on the Ca^{2+} channel have to be occupied for channel opening. The opening and closing of the channel under physiological conditions are limited by the ligand-binding and dissociation steps.

Figure 5 shows the basic features of this model. At equilibrium, a fraction $c/(c + K_D)$ of individual sites are occupied by IP_3 and the kinetics for ligand binding to a single site can be described by $1 - \exp[-(k_{on}c + k_{off})]$. To keep the expression for the opening kinetics simple, we also assume that $k_+ \ll k_-$, implying that the fully liganded channel is open only a small fraction of the time. Because of the assumed independence, the fraction n of open channels at equilibrium is then given by [see also Meyer et al. (1988)]

$$n(c) = k_+/(k_+ + k_-)[c/(c + K_D)]^4 \quad (6)$$

and the channel opening kinetics are given by

$$n(c,t) = n(c)\ [1 - \exp[-(k_{on}c + k_{off})t]]^4 \quad (7)$$

A least-squares fit of the data in Figure 2a gives $K_D = 18$ nM. The on-rate for IP_3 binding, k_{on}, can be obtained from Figure 3. If one binding site would dominate the delay and if $c \gg K_D$, then the delay times for half-maximal opening would be given by $\tau = \tau_0 + 0.69/(k_{on}c)$. A model-independent lower limit for k_{on} of 4.6×10^7 can then be obtained. When four binding sites are used, the delay times are given by $\tau = \tau_0 + 1.84/(k_{on}c)$ (from eq 7). The fit to the points in Figure 3 corresponds to $\tau_0 = 65$ ms and a $k_{on} = 1.2 \times 10^8$ M^{-1} s^{-1}. The value of k_{off} can be determined from $k_{off} = k_{on}K_D$ to be 2.2 s^{-1}. This model gives a good fit of kinetic data obtained over a wide range of IP_3 concentrations (Figures 1–4). However, the present results do not exclude the possibility that the binding sites are heterogeneous or that binding at one site influences binding at another. In fact, because k_{on} is limiting for at least one site down to 15 nM (Figure 3 and eq 6 and 7), at least one binding site has a dissociation constant much less than 18 nM. This could also explain the slower lag time in Figure 4 (factor of $\sim$2) than expected from eq 7. This model is in agreement with the finding by Supattapone et al. (1988) that the IP_3 receptor is a multimer, perhaps a tetramer of 270-kilodalton subunits.

Slowly Dissociating IP_3-Binding Sites. IP_3 binding has been studied in many tissues, and it is interesting to compare the results of these measurements with the IP_3 binding constants of the channel gating site determined from the flux data. Most reported equilibrium binding constants are between 1 nM and 100 nM, and dissociation times are on the order of 100 s [i.e., Spät et al. (1986), Guillemette et al. (1988), and Supattapone et al. (1988)]. The equilibrium binding constants found in these binding studies are comparable to what we infer for the channel gating sites. However, their dissociation times are about 100 times longer than ours. This difference suggests that the sites observed in direct binding assays are not the same as those involved in the opening of Ca^{2+} channels. The rapidly dissociating channel gating sites may not have been observed in previous binding studies because the assays were too slow, or because there are many fewer rapid sites than slow ones. The function of these slow sites is not known. They may regulate the release of Ca^{2+} or they may participate in mediating other processes.

Implications for Cellular Ca^{2+} Homeostasis and Calcium Spiking. Ca^{2+} release follows increases in IP_3 levels after a delay time of the order of several hundred milliseconds. It has been shown that the rising phase of a Ca^{2+} spike during receptor-mediated Ca^{2+} oscillations is also on this time scale (Woods et al., 1986; Jacob et al., 1988; unpublished results in this laboratory). In rapid mixing studies using intact cells and high hormone concentrations, the rise time for the increase in $[Ca^{2+}]$ was a few hundred milliseconds (Sage & Rink, 1987). Our data suggest that the rate-limiting step in both cases was the binding of IP_3 to its receptor. In another informative study (Walker et al., 1987), laser pulse photolysis of caged IP_3 provided information about activation of smooth and skeletal muscle. Their results indicate that Ca^{2+} responses in smooth muscle cells are slow enough to be mediated by IP_3 receptors like those of RBL cells, whereas the much faster Ca^{2+} responses of skeletal muscle are probably mediated in a different way. The large amounts of Ca^{2+} released by IP_3 (corresponding to approximately 1 mM total intracellular Ca^{2+}) and the similarity between rise times for Ca^{2+} spikes and for IP_3-gated Ca^{2+} release support the hypothesis that calcium spiking is driven by rises in intracellular IP_3 concentration (Meyer & Stryer, 1988; Berridge et al., 1988; Cobbold et al., 1989).

Comparison with Other Ligand-Gated Channels. The ligand-binding and channel-opening kinetics of synaptic nicotinic acetylcholine receptor and the cGMP-gated channel from rod outer segments have been determined. Two acetylcholines are required to open the acetylcholine receptor channel (Colquhoun & Sakmann, 1985). The rate constants for the binding of acetylcholine are $\sim 10^8$ M^{-1} s^{-1}, close to the diffusion-controlled limit. A fast ligand dissociation ($\sim 10^4$ s^{-1}, leading to a dissociation constant of $\sim$100 μM) ensures a response time on the order of 100 μs when the concentration of acetylcholine is changed. The intramolecular transition of the closed to the open state was found to be $\sim$33 μs. For the cGMP-gated channel, three or more ligands are required to open the channel (Karpen et al., 1988). The rate constants for binding and dissociation are $\sim 10^8$ M^{-1} s^{-1} and $\sim 10^3$ s^{-1}, respectively, ensuring a response time on the order of 1 ms for changes in cGMP concentration. The intramolecular transition occurs in about $\sim$60 μs. The rate constants for ligand binding and channel opening are matched to the needs of the physiologic signal transduction process. Whereas the synaptic transmission occurs on the time scale of 1 ms and visual transduction on the time scale of 100 ms, hormonal transduction through the phosphoinositide cascade takes place on a slower time scale, of the order of 1 s or longer. It is interesting to note that the on-rate constants are nearly the same ($\sim 10^8$ M^{-1} s^{-1}) for the acetylcholine receptor, the cGMP-gated channel, and the IP_3-gated channel. They differ in their off-rate constants and their equilibrium dissociation constants. Synaptic transmission and visual transduction require faster channels and therefore lower affinity ligand binding and fast off-rate constants. High-affinity ligand-gated channels such as the IP_3-gated Ca^{2+} channel necessarily respond more slowly. A compensating advantage of high affinity is that signal transduction can be achieved with smaller ligand concentration changes and hence a lower expenditure of metabolic energy.

ACKNOWLEDGMENTS

We thank Dr. Jeff Karpen for stimulating discussions.

Registry No. Ca, 7440-70-2; IP_3, 88269-39-0.

REFERENCES

Berridge, M. J. (1987) *Annu. Rev. Biochem. 56*, 159-193.
Berridge, M. J., Cobbold, P. H., & Cuthbertson, K. S. (1988) *Philos. Trans. R. Soc. London, B 320*, 325-343.
Carafoli, E. (1987) *Annu. Rev. Biochem. 56*, 395-433.
Cobbold, P., Daly, M., Dixon, J., & Woods, N. (1989) *Biochem. Soc. Trans. 17*, 9-10.
Colquhoun, D., & Sakmann, B. (1985) *J. Physiol. 369*, 501-557.
Guillemette, G., Balla, T., Baukal, A. J., & Catt, K. J. (1988) *J. Biol. Chem. 263*, 4541-4548.
Jacob, R., Merritt, J. E., Hallam, T. J., & Rink, T. J. (1988) *Nature 355*, 40-45.
Karpen, J. W., Zimmerman, A. L., Stryer, L., & Baylor, D. A. (1988) *Proc. Natl. Acad. Sci. U.S.A. 85*, 1287-1291.
Meyer, T., & Stryer, L. (1988) *Proc. Natl. Acad. Sci. U.S.A. 85*, 5051-5055.
Meyer, T., Holowka, D., & Stryer, L. (1988) *Science 240*, 653-656.
Putney, J. W., Jr. (1987) *Am. J. Physiol. 252*, G149-G157.
Sage, S. O., & Rink, T. J. (1987) *J. Biol. Chem. 262*, 16364-16369.
Spät, A., Bradford, P. G., McKinney, J. S., Rubin, R. P., & Putney, J. W., Jr. (1986) *Nature 319*, 514-516.
Supattapone, S., Worley, J. M., Baraban, S. H., & Snyder, J. (1988) *J. Biol. Chem. 263*, 1530-1536.
Taurog, J. D., Fewtrell, C., & Becker, E. L. (1979) *J. Immunol. 122*, 2150-2153.
Walker, J. W., Somlyo, A. V., Goldman, Y. E., Somlyo, A. P., & Trentham, D. R. (1987) *Nature 327*, 249-252.
Woods, N. M., Cuthbertson, K. S., & Cobbold, P. H. (1986) *Nature 319*, 600-602.

Aminophospholipid Translocation in Erythrocytes: Evidence for the Involvement of a Specific Transporter and an Endofacial Protein†

Jerome Connor and Alan J. Schroit*

Department of Cell Biology, The University of Texas M. D. Anderson Cancer Center, Houston, Texas 77030

Received July 5, 1989; Revised Manuscript Received August 11, 1989

ABSTRACT: The transport of exogenously supplied fluorescent analogues of aminophospholipids from the outer to inner leaflet in red blood cells (RBC) is dependent upon the oxidative status of membrane sulfhydryls. Oxidation of a sulfhydryl on a 32-kDa membrane protein by pyridyldithioethylamine (PDA) has been previously shown [Connor & Schroit (1988) *Biochemistry 27*, 848-851] to inhibit the transport of NBD-labeled phosphatidylserine (NBD-PS). In the present study, other sulfhydryl oxidants were examined to determine whether additional sites are involved in the transport process. Our results show that diamide inhibits the transport of NBD-PS via a mechanism that is independent of the 32-kDa site. This is shown by the inability of diamide to block labeling of the 32-kDa sulfhydryl with ^{125}I-labeled PDA and to protect against PDA-mediated inhibition of NBD-PS transport. Diamide-mediated inhibition, but not PDA-mediated inhibition, could be reversed by reduction with cysteamine or endogenous glutathione. Similarly, treatment of RBC with 5,5′-dithiobis(2-nitrobenzoic acid), which depletes endogenous glutathione and induces oxidation of endofacial proteins [Reglinski et al. (1988) *J. Biol. Chem. 263*, 12360-12366], inhibited NBD-PS transport in a manner analogous to diamide. Once established, the asymmetric distribution of NBD-PS could not be altered by oxidation of either site. These data indicate that a second site critical to the transport of aminophospholipids resides on the endofacial surface and suggest that the transport of aminophospholipids across the bilayer membrane of RBC depends on a coordinated and complementary process between a cytoskeletal component and the 32-kDa membrane polypeptide; both must be operative for transport to proceed.

Phospholipids are asymmetrically distributed in the human erythrocyte membrane (Rothman & Lenard, 1977; Op den Kamp, 1979). In these cells, the aminophospholipids phosphatidylserine (PS)[1] and phosphatidylethanolamine preferentially reside in the inner leaflet, whereas the choline phospholipids are localized in the outer leaflet (Verkleij et al., 1973; Gordesky et al., 1975). This asymmetric organization is maintained through complex and, at present, poorly understood interactions between specific membrane proteins. On the one hand, it has been shown that endofacial proteins such as spectrin (Haest, 1982; Cohen et al., 1986; Maksymiw et al., 1987) and possibly band 4.1 (Sato & Ohnishi, 1983; Rybicki et al., 1988; Cohen et al., 1988; Shiffer et al., 1988) can stabilize PS in the cell's inner leaflet, whereas an ATP-dependent translocase is responsible for the outside to inside

† This work was supported by Grants CA-47845 and DK-41714 from the National Institutes of Health and by Developmental Fund Grant 175416 from The University of Texas M. D. Anderson Cancer Center.
* To whom correspondence should be addressed.

[1] Abbreviations: ^{125}I-PDA, *N*-[3-(3-[^{125}I]iodo-4-hydroxyphenyl)-propionyl]pyridyldithioethylamine (Bolton-Hunter-labeled PDA); DOPC, dioleoylphosphatidylcholine; DTNB, 5,5′-dithiobis(2-nitrobenzoic acid) (Ellman's reagent); DTT, dithiothreitol; GSH, reduced glutathione; GSSG, oxidized glutathione; NBD-PS, 1-oleoyl-2-[[*N*-(7-nitro-2,1,3-benzoxadiazol-4-yl)amino]caproyl]phosphatidylserine; PBS, phosphate-buffered saline (137 mM NaCl, 3 mM KCl, 10 mM sodium/potassium phosphates, and 10 mM glucose, pH 7.4); NEM, *N*-ethylmaleimide; PC, phosphatidylcholine; PDA, pyridyldithioethylamine; PS, phosphatidylserine; RBC, red blood cell(s); SDS, sodium dodecyl sulfate; SDS-PAGE, SDS-polyacrylamide gel electrophoresis.

0006-2960/90/0429-37$02.50/0